PHYSICAL REVIEW D 76, 094504 (2007)

Scalar meson spectroscopy with lattice staggered fermions

Claude Bernard
Physics Department, Washington University, St. Louis, Missouri 63130, USA

Carleton DeTar and Ziwen Fu
Physics Department, University of Utah, Salt Lake City, Utah 84112, USA

Sasa Prelovsek
Department of Physics, University of Ljubljana, Jadranska 19, Ljubljana, Slovenia
and J. Stefan Institute, Jamova 39, Ljubljana, Slovenia
(Received 18 July 2007; published 7 November 2007)

With sufficiently light up and down quarks the isovector (a_0) and isosinglet (f_0) scalar meson propagators are dominated at large distance by two-meson states. In the staggered-fermion formulation of lattice quantum chromodynamics, taste-symmetry breaking causes a proliferation of two-meson states that further complicates the analysis of these channels. Many of them are unphysical artifacts of the lattice approximation. They are expected to disappear in the continuum limit. The staggered-fermion fourth-root procedure has its purported counterpart in rooted staggered chiral perturbation theory (rSχPT). Fortunately, the rooted theory provides a strict framework that permits the analysis of scalar meson correlators in terms of only a small number of low-energy couplings. Thus the analysis of the point-to-point scalar meson correlators in this context gives a useful consistency check of the fourth-root procedure and its proposed chiral realization. Through numerical simulation we have measured correlators for both the a_0 and f_0 channels in the "Asqtad" improved staggered-fermion formulation in a lattice ensemble with lattice spacing $a = 0.12$ fm. We analyze those correlators in the context of rSχPT and obtain values of the low-energy chiral couplings that are reasonably consistent with previous determinations.

DOI: 10.1103/PhysRevD.76.094504 PACS numbers: 11.15.Ha, 12.38.Gc, 12.39.Fe, 14.40.Cs

I. INTRODUCTION

The recent evident successes of numerical simulations of QCD with improved staggered fermions demand a thorough examination of its most controversial ingredient, namely, using fractional powers of the determinant to simulate the correct number of quark species (the "fourth-root trick"). The procedure is known to introduce nonlocalities and violations of unitarity at nonzero lattice spacing [1]. If these problems do not vanish in the continuum limit, they may even place the theory in an unphysical universality class. There are, however, strong theoretical arguments [2–5] that the fourth-root trick is valid, i.e. that it produces QCD in the continuum limit.

One may also test the fourth-root procedure numerically. One can, for example, check that taste symmetry gets restored as the lattice spacing gets smaller, by looking at the eigenvalue spectrum [6–10], the Dirac operator [11], or the pion spectrum [12]. Alternatively, low-energy results of staggered-fermion QCD simulations can be compared with predictions of rooted staggered chiral perturbation theory (rSχPT) [13,14]. Since staggered chiral perturbation theory becomes standard chiral perturbation theory in the continuum limit, agreement between rooted QCD and (rSχPT) at nonzero lattice spacing would suggest that, at least for low-energy or long-range phenomena, lattice artifacts produced by the fourth-root approximation are as harmless as those produced by partial quenching. Partial quenching also induces unitarity violations, but they disappear in the limit of equal valence and sea quark masses.

There are two recent tests of agreement between rooted staggered-fermion QCD and rSχPT: (1) Measurements of the light pseudoscalar meson masses and decay constants in partially quenched and full staggered-fermion QCD fit well to expressions derived from rSχPT [15]. A byproduct of this fit is a determination of the low-energy couplings of the theory. (2) The topological susceptibility measured in full QCD agrees reasonably well with predictions of rSχPT [16].

In the present work we examine scalar meson correlators in full QCD and compare their two-meson content with predictions of rSχPT. Since the appearance of the two-meson intermediate state is a consequence of the fermion determinant, an analysis of this correlator provides a direct test of the fourth-root recipe. The a_0 channel has been studied recently in staggered-fermion QCD by the MILC collaboration [17] and UKQCD collaboration [18]. Both groups found that the correlator appeared to contain states with energies well below possible combinations of physical mesons.

A simple explanation of the nonstandard features of the scalar correlators is provided by rSχPT [19,20]. In that theory all pseudoscalar mesons come in multiplets of 16 tastes. The pattern of mass splittings is predicted by the theory. The π and K multiplets are split in similar ways. The η and η' mesons, however, are peculiar, because their

masses are shifted by the axial $U(1)$ anomaly. Since the anomaly is a taste singlet, only the taste singlet η and η' acquire approximately physical masses. Some of the remaining members of the η multiplet remain degenerate with the pions. According to taste-symmetry selection rules, any two mesons coupling to a taste singlet a_0 must have the same taste. But all tastes are equally allowed. Among other states, the taste singlet a_0 couples to the Goldstone pion (pseudoscalar taste) and an η, also with pseudoscalar taste and of the same mass. This spurious two-body state at twice the mass of the Goldstone boson accounts for the anomalous low-energy component in that channel.

This explanation raises concerns. Clearly, only the taste singlet η approximates the physical state, since it is the only member of the multiplet subject to the anomaly. So if the other η's are not allowed as external states, we have violated unitarity in the sense that some intermediate states are not allowed as external states. Further examination of the taste multiplets in the intermediate states reveals that in addition to the several unphysical $\pi\eta$ taste combinations, there is a negative norm "ghost" contribution in the taste singlet η meson leg [21]. Remarkably, all lattice artifacts resolve themselves in the continuum limit, however [22]. The taste multiplets become degenerate, the two-body states merge, and the ghost state cancels the spurious taste combinations, leaving only the taste-singlet mesons. To achieve this cancellation requires following the rules of flavor counting in rSχPT.

In the present work we extend the analysis of Refs. [19,20] and carry out a quantitative comparison of measured correlators and predictions of rSχPT. Despite the considerable complexity of channels with dozens of spectral components, the chiral theory models the correlators precisely in terms of only a small number of low-energy couplings, which we may determine through fits to the data.

This article is organized as follows. Following a review of some needed results from SχPT in Sec. II, we derive the chiral predictions for the a_0 and f_0 in Sec. III. We present results of our fits to the predicted forms in Sec. IV and conclude in Sec. V.

II. ELEMENTS OF STAGGERED CHIRAL PERTURBATION THEORY

In this section we give a brief review of rooted staggered chiral perturbation theory with particular emphasis on the tree-level pseudoscalar mass spectrum. We obtain the rooted version of the theory through the replica trick, according to which each quark flavor, u, d, and s, comes in four tastes and is repeated n_r times [23]. We calculate various quantities in the replicated theory, and in the final step, we set $n_r = 1/4$ to obtain the correct flavor counting.

The low-energy effective chiral theory is formulated in terms of the meson field

$$\Phi = \sum_{b=1}^{16} \frac{1}{2} T^b \phi^b, \tag{1}$$

where $T^b = \{1, \xi_5, i\xi_5\xi_\mu \ldots\}$ are Dirac gamma matrices and ϕ^b is a $3n_r \times 3n_r$ matrix with rows and columns labeled by the flavor and replica index ur, dr, and sr. The staggered chiral action is written in terms of the unitary matrix $\Sigma = \exp(2i\Phi/f)$:

$$S(\Sigma, m) = \int d^4y \left\{ \frac{f^2}{8} \mathrm{Tr}(\partial_\mu \Sigma^\dagger \partial^\mu \Sigma) - \frac{\mu f^2}{4} \mathrm{Tr}(\mathcal{M}\Sigma^\dagger + \mathcal{M}^\dagger \Sigma) + \frac{m_0^2}{2} \phi_{0I}^2 + a^2 \mathcal{V}(\Sigma) \right\}. \tag{2}$$

The low-energy couplings at this order are f, μ, and the quark mass matrix $\mathcal{M} = I_t \otimes I_r \mathrm{diag}(\mathrm{m_u}, \mathrm{m_d}, \mathrm{m_s})$, where I_t is the unit matrix in taste space and I_r is the unit matrix in replica space. The axial anomaly appears through the mass term m_0^2. It involves the flavor-singlet taste-singlet field $\phi_{0I} = \sum_{f,r} \phi^I_{fr,fr}/\sqrt{3n_r}$. The taste-breaking term $\mathcal{V}$ is a linear combination of operators [13,14,24]

$$-\mathcal{V}(\Sigma) = \sum C_i \mathcal{O}_i, \tag{3}$$

where

$$\mathcal{O}_1 = \mathrm{Tr}(T_{0,5}\Sigma T_{0,5}\Sigma^\dagger), \tag{4}$$

$$\mathcal{O}_{2V} = \tfrac{1}{4}[\mathrm{Tr}(T_{0,\mu}\Sigma)\mathrm{Tr}(T_{0,\mu}\Sigma) + \mathrm{H.c.}], \tag{5}$$

$$\mathcal{O}_{2A} = \tfrac{1}{4}[\mathrm{Tr}(T_{0,\mu 5}\Sigma)\mathrm{Tr}(T_{0,5\mu}\Sigma) + \mathrm{H.c.}], \tag{6}$$

$$\mathcal{O}_3 = \tfrac{1}{2}[\mathrm{Tr}(T_{0,\mu}\Sigma T_{0,\mu}\Sigma) + \mathrm{H.c.}], \tag{7}$$

$$\mathcal{O}_4 = \tfrac{1}{2}[\mathrm{Tr}(T_{0,\mu 5}\Sigma T_{0,5\mu}\Sigma) + \mathrm{H.c.}], \tag{8}$$

$$\mathcal{O}_{5V} = \tfrac{1}{2}[\mathrm{Tr}(T_{0,\mu}\Sigma)\,\mathrm{Tr}(T_{0,\mu}\Sigma^\dagger)], \tag{9}$$

$$\mathcal{O}_{5A} = \tfrac{1}{2}[\mathrm{Tr}(T_{0,\mu 5}\Sigma)\,\mathrm{Tr}(T_{0,5\mu}\Sigma^\dagger)], \tag{10}$$

$$\mathcal{O}_6 = \sum_{\mu<\nu} \mathrm{Tr}(T_{0,\mu\nu}\Sigma T_{0,\nu\mu}\Sigma^\dagger). \tag{11}$$

Without the anomaly and taste-breaking term the tree-level masses of the pseudoscalar mesons with quark flavor content f, f' are, as usual,

$$M^2_{f,f',b} = \mu(m_f + m_{f'}). \tag{12}$$

The taste-breaking term splits the nonisosinglet states (π_b and K_b) to give

$$M^2_{f,f',b} = \mu(m_f + m_{f'}) + a^2\Delta_b, \tag{13}$$

where to leading order the multiplets split five ways,

$$\begin{aligned}\Delta_5 &= 0,\\ \Delta_{\mu 5} &= \frac{16}{f^2}(C_1 + 3C_3 + C_4 + 3C_6),\\ \Delta_{\mu\nu} &= \frac{16}{f^2}(2C_3 + 2C_4 + 4C_6),\\ \Delta_{\mu} &= \frac{16}{f^2}(C_1 + C_3 + 3C_4 + 3C_6),\\ \Delta_I &= \frac{16}{f^2}(4C_3 + 4C_4),\end{aligned} \tag{14}$$

which we label P, A, T, V, and I, respectively. This predicted multiplet pattern has been well confirmed in simulations [17,25].

We will be working with degenerate u and d quarks ($m_u = m_d = m_\ell$), so it will be convenient to introduce the notation

$$\begin{aligned}M_{Ub}^2 = 2\mu m_\ell + a^2\Delta_b, \qquad M_{Sb}^2 = 2\mu m_s + a^2\Delta_b,\\ M_{Kb}^2 = \mu(m_\ell + m_s) + a^2\Delta_b.\end{aligned} \tag{15}$$

The isosinglet states (η and η') are modified both by the taste-singlet anomaly and by the two-trace (quarkline hairpin) taste-vector and taste-axial-vector operators $\mathcal{O}_{2V}$, $\mathcal{O}_{2A}$, $\mathcal{O}_{5V}$, and $\mathcal{O}_{5A}$. When m_0^2 is large, in the taste-singlet sector we obtain the usual result

$$M_{\eta,I}^2 = \tfrac{1}{3}M_{UI}^2 + \tfrac{2}{3}M_{SI}^2, \qquad M_{\eta',I} = \mathcal{O}(m_0^2). \tag{16}$$

In the taste-axial-vector sector we have

$$\begin{aligned}M_{\eta A}^2 &= \tfrac{1}{2}[M_{UA}^2 + M_{SA}^2 + 3n_r\delta_A - Z_A],\\ M_{\eta' A}^2 &= \tfrac{1}{2}[M_{UA}^2 + M_{SA}^2 + 3n_r\delta_A + Z_A],\\ Z_A^2 &= (M_{SA}^2 - M_{UA}^2)^2 - 2n_r\delta_A(M_{SA}^2 - M_{UA}^2) + 9n_r^2\delta_A^2,\end{aligned} \tag{17}$$

where $\delta_A = a^2\delta'_A = a^2 16(C_{2A} - C_{5A})/f^2$, and likewise for $A \to V$.

In the taste-pseudoscalar and taste-tensor sectors, in which is there is no mixing of the isosinglet states, the η_b and η'_b by definition have quark content $(\bar{u}u + \bar{d}d)/\sqrt{2}$ and $\bar{s}s$, respectively, and masses

$$M_{\eta,b}^2 = M_{Ub}^2; \qquad M_{\eta',b}^2 = M_{Sb}^2. \tag{18}$$

TABLE I. Masses of pseudoscalar meson taste multiplets in lattice units for the MILC coarse ($a = 0.12$ fm) lattice ensemble $\beta = 6.76$, $am_{ud} = 0.005$, $am_s = 0.05$, as measured or inferred from measured masses and splittings. The mass of the η'_I depends on the anomaly parameter m_0.

b	π_b	K_b	η_b	η'_b
P	0.1594	0.3652	0.1594	0.4927
A	0.2342	0.4036	0.1843	0.5129
T	0.2694	0.4250	0.2694	0.5384
V	0.2966	0.4428	0.2825	0.5491
I	0.3205	0.4592	0.4958	—

In Table I we list the masses of the resulting taste multiplets for the lattice ensemble used in the present study with taste-breaking parameters δ_A and δ_V determined in Refs. [15,17].

III. SCALAR CORRELATORS FROM SχPT

In this section we rederive the "bubble" contribution to the a_0 channel of Ref. [20], using the language of the replica trick [13,26], and then extend the result to the f_0 channel.

We match the point-to-point scalar correlators in chiral low-energy effective theory and staggered-fermion QCD by matching the Green's functions, which are defined through the generating functionals of the respective theories:

$$\frac{\partial^2 \log Z}{\partial m_{f,f'}(y)\partial m_{e',e}(0)}. \tag{19}$$

For this purpose the quark mass term diag(m_u, m_d, m_s) is converted to a local meson source $m_{ff'}(y)$ (including flavor off-diagonal terms) in both SχPT and QCD.

A. Scalar correlator in staggered-fermion QCD

First we review the construction of the needed correlators in staggered lattice QCD, where the generating functional is

$$Z(m_{ff'}) = \int dU \exp[-S_g(U)]\det[M(U, m_{ff'})]^{1/4}. \tag{20}$$

Here U are the gauge link variables, $S_g(U)$ is the gauge action, and M is the fermion matrix including flavor components. We work on a lattice of spacing a and dimension $L^3 \times N_t$ and label sites by the integer four-vector x_μ. Hypercubes of size 2^4 are similarly labeled by y_μ, so $x_\mu = 2y_\mu + \eta_\mu$.

Staggered-fermion meson correlators can be defined in the one-component basis of the Grassman color vector field $\chi_f(x)$ or in the spin-taste basis of the field $q_f^{a\alpha}(y)$ with spin label α and taste label a. The fields are related through

$$\begin{aligned}q_f^{a\alpha}(y) &= \frac{1}{8}\sum_\eta \Gamma_\eta^{a\alpha}\chi_f(2y + \eta),\\ \chi_f(2y + \eta) &= 2\,\mathrm{Tr}[\Gamma_\eta^\dagger q_f(y)],\end{aligned} \tag{21}$$

where $\Gamma_\eta = \gamma_0^{\eta_0}\gamma_1^{\eta_1}\gamma_2^{\eta_2}\gamma_3^{\eta_3}$, and the sum over η runs over sites in the 2^4 hypercube labeled by y. The lattice y has spacing $A = 2a$.

For constructing the meson correlators via the functional derivative (19) we need to introduce the source term into Lagrangian

$$S_m = a^4 \sum_x \bar{\chi}_f(x)\chi_{f'}(x) m_{f,f'}(x). \quad (22)$$

To express the source in terms of the spin-taste basis we use the relation

$$a^4 \bar{\chi}_f(2y+\eta)\chi_{f'}(2y+\eta) = \frac{A^4}{16}\sum_\Gamma \zeta(\Gamma,\eta)\rho_{f,f',\Gamma}(y) \quad (23)$$

with

$$\zeta(\Gamma,\eta) = \mathrm{Tr}(\Gamma_\eta^\dagger \Gamma^\dagger \Gamma_\eta \Gamma)/4 \quad (24)$$

and

$$\rho_{f,f',\Gamma}(y) = \bar{q}_f(y)\Gamma \otimes \Gamma^* q_{f'}(y). \quad (25)$$

The direct product $\Gamma_S \otimes \Gamma_T^*$ acts on spin and taste components, respectively. So we obtain

$$S_m = A^4 \sum_{y,\Gamma} \rho_{f,f',\Gamma}(y) m_{f,f',\Gamma}(y) \quad (26)$$

with

$$m_{f,f',\Gamma}(y) = \frac{1}{16}\sum_\eta \zeta(\Gamma,\eta) m_{f,f'}(2y+\eta). \quad (27)$$

The desired source for the scalar density, $m_{f,f',I}(y)$, has $\Gamma = I$ and $\zeta(I,\eta) = 1$. It is the component of $m_{f,f'}(x)$ that is constant over a 2^4 hypercube. The other terms $m_{f,f',\Gamma}(y)$ are sources for the other local staggered mesons.

A particular correlator is obtained by differentiating the generating functional with respect to the appropriate source mass terms. The general two-point function is, then,

$$\frac{\partial^2 \log Z}{\partial m_{f,f',\Gamma}(y)\partial m_{e',e,\Gamma'}(0)}\bigg|_{m_{jj'}(x)=\delta_{jj'}m_j} = A^8 \langle \bar{\rho}_{f,f',\Gamma}(y)\rho_{e',e,\Gamma'}(0)\rangle. \quad (28)$$

The above quantity will be calculated for $\Gamma = I$ also within SχPT below.

Now, we need to relate the quantity (28) to the correlator generated from the code. In practice the simulated correlator is computed from a point source at the origin

$$O_{e,e',\mathrm{src}} = a^3 \bar{\chi}_{e'}(0)\chi_e(0) = \frac{A^3}{8}\sum_\Gamma \rho_{e,e'\Gamma}(0), \quad (29)$$

and a single time slice sink operator at time $\tau = 2t + \eta_0$,

$$O_{f,f'\mathrm{sink}}(\vec{y},\tau) = a^3 \sum_{\vec{\eta}} \bar{\chi}_{f'}(2\vec{y}+\vec{\eta},\tau)\chi_f(2\vec{y}+\vec{\eta},\tau) = A^3[\rho_{f,f',I}(2\vec{y},t) + (-)^{\eta_0}\rho_{f,f',05}(2\vec{y},t)], \quad (30)$$

where we have used relation (23), $\zeta(I,\eta) = 1$, and $\zeta(05,\eta) = (-)^{\eta_0}$. Note that the sink operator is defined on spatial cubes $\vec{y}$ but all time slices τ.

In this language the computed correlator is

$$C_{f,f';e,e'}(\vec{p},\tau a) = \sum_{\vec{y}} \exp(i\vec{p}\cdot\vec{y}A)\langle \bar{O}_{f,f'\mathrm{sink}}(\vec{y},\tau) O_{e,e'\mathrm{src}}\rangle. \quad (31)$$

The meson taste is conserved, so the correlator separates into nonoscillating and oscillating components for a taste-singlet scalar contribution and a taste-axial-vector pseudoscalar meson contribution, respectively.

$$C_{f,f';e,e'}(\vec{p},\tau a) = C_{f,f';e,e',I}(\vec{p},\tau a) + (-)^\tau C_{f,f';e,e',05}(\vec{p},\tau a), \quad (32)$$

where

$$C_{f,f';e,e',\Gamma}(\vec{p},\tau a) = \frac{A^6}{8}\sum_{\vec{y}} \exp(i\vec{p}\cdot\vec{y}A) \times \langle \rho_{f,f',\Gamma}(2\vec{y},t)\rho_{e,e',\Gamma}(0)\rangle. \quad (33)$$

The correlator has a quark-line-connected part and may also have a quarkline disconnected part:

$$C_{f,f';e,e',\Gamma}(\vec{p},\tau a) = C_{f,f';e,e',\Gamma,\mathrm{conn}}(\vec{p},\tau a) + C_{f,f';e,e',\Gamma,\mathrm{disc}}(\vec{p},\tau a). \quad (34)$$

The quarkline disconnected part appears only in the taste-singlet isosinglet correlator.

To compute the correlator we need to express it in terms of quark propagators. So we start from the definition of the correlator in Eq. (31), substitute the definitions of the operators in Eqs. (29) and (30), and use the relation

$$a^8\langle \bar{\chi}_f(2y+\eta)\chi_{f'}(2y+\eta)\bar{\chi}_e(\eta')\chi_{e'}(\eta')\rangle = \frac{\partial^2 \log Z}{\partial m_{f,f'}(2y+\eta)\partial m_{e',e}(\eta')}\bigg|_{m_{jj'}(x)=\delta_{jj'}m_j} = \frac{A^8}{256}\sum_{\Gamma,\Gamma'} \zeta(\Gamma,\eta)\zeta(\Gamma',\eta')\langle \bar{\rho}_{f,f',\Gamma}(y)\rho_{e',e,\Gamma'}(0)\rangle, \quad (35)$$

which follows from the identity

$$\frac{\partial}{\partial m(2y+\eta)} = \frac{1}{16}\sum_\Gamma \zeta(\Gamma,\eta)\frac{\partial}{\partial m_\Gamma(y)}. \quad (36)$$

Finally we arrive at the point-to-point correlators

$$C_{f,f';e,e',\mathrm{conn}}(\vec{p},\tau a) = -\sum_{\vec{x}}(-)^x \exp(i\vec{p}\cdot\vec{x}a) \times \langle \mathrm{Tr}[M_f^{-1}(\vec{x},\tau;0,0) \times M_{f'}^{-1\dagger}(\vec{x},\tau;0,0)]\rangle \delta_{ef}\delta_{e'f'},$$

$$C_{f,f';e,e',\mathrm{disc}}(\vec{p},\tau a) = \frac{1}{4}\sum_{\vec{x}} \exp(i\vec{p}\cdot\vec{x}a) \times \langle \mathrm{Tr}[M_f^{-1}(\vec{x},\tau;\vec{x},\tau)] \times \mathrm{Tr}[M_e^{-1\dagger}(0,0;0,0)]\rangle \delta_{ee'}\delta_{ff'},$$

where we have used Eq. (20) and the normalization $M = 2D + 2am$ for the Dirac matrix. We keep the momentum p small, so we can neglect variation of the exponential over the hypercube.

As it is computed, at zero momentum the quarkline disconnected correlator includes the vacuum disconnected piece:

$$C_{f,e,0} = \frac{L^3}{4}\langle \mathrm{Tr}[M_f^{-1}(0,0;0,0)]\rangle\langle \mathrm{Tr}[M_e^{-1}(0,0;0,0)]\rangle. \quad (37)$$

B. Scalar correlator in SχPT

The continuum generating functional for scalar correlators in SχPT

$$Z_{\mathrm{SXPT}}(m_{ff'}) = \int [d\Sigma] \exp[-S(\Sigma, m_{ff'})], \quad (38)$$

where $S(\Sigma, m_{ff'})$ is given by Eq. (2). We do not include explicit scalar meson fields in the chiral Lagrangian, but add their contributions in the final expressions. To match the functional derivatives (19) we approximate the continuum integration in the chiral theory with a sum over hypercubic volumes of size A^4 and differentiate with respect to a constant source inside that volume. In this case $m_{f,f',I}(y) = m_{f,f'}(y)$. The source is also constant over replicas of the same flavor. The space-time volume equals that of QCD, namely, $A^4(L/2)^3 N_t/2$ for $A = 2a$. We use the integer four-vector y to label the hypercubes in the chiral theory. The functional derivative in SχPT is

$$\frac{\partial^2 \log Z_{\mathrm{SXPT}}}{\partial m_{f,f'}(y)\partial m_{e',e}(0)} = A^8\mu^2 \sum_{r,r'} \langle \mathrm{Tr}_t(\Phi^2(y))_{fr,f'r}\,\mathrm{Tr}_t(\Phi^2(0))_{er',e'r'}\rangle. \quad (39)$$

At tree level the action (2) has no explicit quark-antiquark scalar meson fields, but it generates the two-pseudoscalar-meson bubble terms in the correlator. The functional derivative (39) corresponds to (28) with $\Gamma = I$. We use B to denote the bubble contribution corresponding to the correlator (33)

$$B_{f,f';e,e',I}(\vec{p}, tA) = \frac{A^6}{8}\sum_{\vec{y}} \exp(i\vec{p}\cdot\vec{y}A)\langle \rho_{f,f',I}(y)\rho_{e,e',I}(0)\rangle = \frac{A^6}{8}\sum_{\vec{y}} \exp(i\vec{p}\cdot\vec{y}A)\mu^2 \times \sum_{r,r'}\langle \mathrm{Tr}_t(\Phi^2(y))_{fr,f'r}\,\mathrm{Tr}_t(\Phi^2(0))_{er',e'r'}\rangle. \quad (40)$$

We introduce its time Fourier transform

$$B_{f,f';e,e',I}(p) = \sum_{t=0}^{N_t/2} \exp(ip_0 tA) B_{f,f';e,e',I}(\vec{p}, tA). \quad (41)$$

At tree level the vacuum expectation value reduces through Wick contractions to products of meson two-point functions. In momentum space we have, generically, the Euclidean correlator

$$\langle \phi(y)\phi(0)\rangle = \frac{1}{A^4(L/2)^3(N_t/2)}\sum_k \exp(ik\cdot yA) \times \langle \phi(-k)\phi(k)\rangle, \quad (42)$$

where $\langle \phi(-k)\phi(k)\rangle = 1/(k^2 + m^2)$. So

$$\langle \phi(y)\phi(0)\rangle = \frac{1}{A^3(L/2)^3}\sum_{\vec{k}} \frac{\exp[-E(\vec{k})tA + i\vec{k}\cdot\vec{y}A]}{2E(\vec{k})} \quad (43)$$

for $E(\vec{k}) = \sqrt{|\vec{k}|^2 + m^2}$. In terms of momentum components, the general term in the correlator becomes

$$B_{f,f';e,e',I}(p) = \frac{A^6\mu^2}{8}\sum_y \exp(ip\cdot yA)\sum_{g,s,r,b}\sum_{g',s',r',b'}\langle \phi^b_{fr,gs}(\vec{y},t)\phi^b_{gs,f'r}(\vec{y},t)\phi^{b'}_{er',g's'}(0)\phi^{b'}_{g's'e'r'}(0)\rangle = \frac{\mu^2}{8(L/2)^3(N_t/2)A^2}\sum_k \sum_{g,s,r,b}\sum_{g',s',r',b'}[\langle \phi^b_{fr,gs}(-k)\phi^{b'}_{er',g's'}(k)\rangle\langle \phi^b_{gs,f'r}(k-p)\phi^{b'}_{g's'e'r'}(p-k)\rangle + \langle \phi^b_{fr,gs}(-k)\phi^{b'}_{g's'e'r'}(k)\rangle\langle \phi^b_{gs,f'r}(k-p)\phi^{b'}_{er',g's'}(p-k)\rangle]. \quad (44)$$

We have used the fact that the bubble term, by definition, does not include the vacuum disconnected piece corresponding to Eq. (37).

There are two types of two-point functions, namely, the connected two-point function for all tastes:

$$\langle \phi^b_{gs,fr}(-k)\phi^b_{f'r',g's'}(k)\rangle_{\mathrm{conn}} = \frac{\delta_{r,r'}\delta_{f,f'}\delta_{g,g'}\delta_{s,s'}}{k^2 + M^2_{fg,b}}, \quad (45)$$

and the additional disconnected contribution for the taste-singlet, taste-axial-vector, and taste-vector mesons. For the taste singlet it is

$$\langle \phi^I_{gs,fr}(-k)\phi^I_{f'r',g's'}(k)\rangle_{\mathrm{disc}} = -\frac{\delta_{r,s}\delta_{r',s'}\delta_{f,g}\delta_{f',g'}}{3n_r} \times \frac{k^2 + M^2_{SI}}{(k^2 + M^2_{UI})(k^2 + M^2_{\eta I})}. \quad (46)$$

Here we have already decoupled the taste singlet η' by taking $m_0^2 \to \infty$. The disconnected contribution for the taste-axial-vector meson is

$$\langle \phi^A_{gs,fr}(-k)\phi^A_{f'r',g's'}(k)\rangle_{\rm disc} = -\delta_{r,s}\delta_{r',s'}\delta_{f,g}\delta_{f',g'} \times \frac{\delta_A(k^2+M^2_{SA})}{(k^2+M^2_{UA})(k^2+M^2_{\eta A})(k^2+M^2_{\eta' A})}, \quad (47)$$

and there is a similar contribution for the taste-vector meson.

It is convenient to carry out a partial fraction expansion of the disconnected contributions as follows:

$$\langle \phi^I_{gs,fr}(-k)\phi^I_{f'r',g's'}(k)\rangle_{\rm disc} = -\frac{\delta_{r,s}\delta_{r',s'}\delta_{f,g}\delta_{f',g'}}{3n_r} \times \left(\frac{3/2}{k^2+M^2_{UI}} - \frac{1/2}{k^2+M^2_{\eta I}}\right) \quad (48)$$

and

$$\langle \phi^A_{gs,fr}(-k)\phi^A_{f'r',g's'}(k)\rangle_{\rm disc} = -\delta_{r,s}\delta_{r',s'}\delta_{f,g}\delta_{f',g'}\delta_A \times \left(\frac{g_U}{k^2+M^2_{UA}} + \frac{g_\eta}{k^2+M^2_{\eta A}} + \frac{g_{\eta'}}{k^2+M^2_{\eta' A}}\right), \quad (49)$$

where

$$g_U = \frac{M^2_{SA}-M^2_{UA}}{(M^2_{\eta A}-M^2_{UA})(M^2_{\eta' A}-M^2_{UA})}, \quad g_\eta = \frac{M^2_{SA}-M^2_{\eta A}}{(M^2_{UA}-M^2_{\eta A})(M^2_{\eta' A}-M^2_{\eta A})}, \quad g_{\eta'} = \frac{M^2_{SA}-M^2_{\eta' A}}{(M^2_{UA}-M^2_{\eta' A})(M^2_{\eta A}-M^2_{\eta' A})}. \quad (50)$$

In the language of Refs. [13,14], g_U, g_η, and $g_{\eta'}$ are simply the residues for Eq. (47). Similarly, the factors of $3/2$ and $-1/2$ in Eq. (48) are the residues for Eq. (46).

C. Isovector a_0 correlator

We now specialize to the isovector a_0 correlator. We consider, for simplicity, the $u\bar{d}$ flavor state. Only the quark-line-connected contribution appears in the QCD correlator

$$B_{a_0}(\vec{p},\tau a) = B_{u,d;d,u}(\vec{p},\tau a) = -\sum_{\vec{x}}(-)^x \exp(i\vec{p}\cdot\vec{x}) \times \langle {\rm Tr}[M_u^{-1}(\vec{x},\tau;0,0)M_d^{-1\dagger}(\vec{x},\tau;0,0)]\rangle. \quad (51)$$

In terms of the meson fields, the bubble correlator is (for $\tau a = tA$)

$$B_{u,d;u,d,I}(\vec{p},tA) = \frac{A^6\mu^2}{8}\sum_{\vec{y}}\exp(i\vec{p}\cdot\vec{y}A) \times \sum_{r,s,f,b}\sum_{r',s',f',b'}\langle \phi^b_{ur,fs}(\vec{y},t) \times \phi^b_{fs,dr}(\vec{y},t)\phi^{b'}_{dr',f's'}(0)\phi^{b'}_{f's',ur'}(0)\rangle. \quad (52)$$

After carrying out the Wick contractions and switching to momentum space we get

$$B_{a_0}(p) = \frac{\mu^2}{8A^2(L/2)^3(N_t/2)}\left\{n_r^2\sum_{f,b}\sum_k\left[\frac{1}{k^2+M^2_{fu,b}}\frac{1}{(k+p)^2+M^2_{fu,b}}\right] - 4n_r\sum_k\left[\frac{1}{(k+p)^2+M^2_{UI}}\frac{1}{3n_r} \times \frac{k^2+M^2_{SI}}{(k^2+M^2_{UI})(k^2+M^2_{\eta I})}\right] - 4n_r\sum_k\left[\frac{4\delta_A}{(k+p)^2+M^2_{UA}}\frac{k^2+M^2_{SA}}{(k^2+M^2_{UA})(k^2+M^2_{\eta A})(k^2+M^2_{\eta' A})}\right] - 4n_r\sum_k\left[\frac{4\delta_V}{(k+p)^2+M^2_{UV}}\frac{k^2+M^2_{SV}}{(k^2+M^2_{UV})(k^2+M^2_{\eta V})(k^2+M^2_{\eta' V})}\right]\right\}. \quad (53)$$

Notice, in particular, the negative weight threshold in the second term and the spurious taste nonsinglet $\pi\eta$ thresholds involving Goldstone-boson-like members of the η taste multiplet.

In the continuum limit, in which taste symmetry is restored, we have

$$B_{a_0}(p) = \frac{\mu^2}{8A^2(L/2)^3(N_t/2)}\left\{16n_r^2\sum_f\sum_k\left[\frac{1}{k^2+M^2_{fu}}\frac{1}{(k+p)^2+M^2_{fu}}\right] - \frac{4}{3}\sum_k\left[\frac{1}{(k+p)^2+M^2_U}\frac{k^2+M^2_S}{(k^2+M^2_U)(k^2+M^2_\eta)}\right]\right\}.$$

Here the total contribution from pairs of light states with mass M_U is proportional to

$$(32n_r^2 - 2), \quad (54)$$

which vanishes when $n_r = 1/4$. The negative-norm threshold has neatly canceled the unphysical thresholds. The surviving thresholds are the physical $\bar{K}K$ and taste singlet $\pi\eta$.

D. Isosinglet f_0 correlator

In this case we use the isosinglet operator $(\rho_{uu,I} + \rho_{dd,I})/\sqrt{2}$. We have both quark-line-connected and quark-line-disconnected contributions

$$B_{f_0}(\vec{p}, \tau a) = B_{f_0,\mathrm{conn}}(\vec{p}, \tau a) + B_{f_0,\mathrm{disc}}(\vec{p}, \tau a), \tag{55}$$

$$\begin{aligned} B_{f_0,\mathrm{conn}}(\vec{p}, \tau a) &= \frac{1}{2}[B_{u,u;u,u,\mathrm{conn}}(\vec{p}, \tau a) + B_{d,d;d,d,\mathrm{conn}}(\vec{p}, \tau a)] \\ &= -\sum_{\vec{x}} (-)^x \exp(i\vec{p}\cdot\vec{x}a)\langle \mathrm{Tr}[M_u^{-1}(\vec{x}, \tau; 0, 0) \\ &\quad \times M_u^{-1\dagger}(\vec{x}, \tau; 0, 0)]\rangle, \end{aligned} \tag{56}$$

$$\begin{aligned} B_{f_0,\mathrm{disc}}(\vec{p}, \tau a) &= \frac{1}{2}[B_{u,u;u,u,\mathrm{disc}}(\vec{p}, \tau a) + B_{u,u;d,d,\mathrm{disc}}(\vec{p}, \tau a) \\ &\quad + B_{d,d;u,u,\mathrm{disc}}(\vec{p}, \tau a) + B_{d,d;d,d,\mathrm{disc}}(\vec{p}, \tau a)] \\ &= \frac{1}{2}\sum_{\vec{x}} \exp(i\vec{p}\cdot\vec{x}a)\langle \mathrm{Tr}[M_u^{-1}(\vec{x}, \tau; \vec{x}, \tau)] \\ &\quad \times \mathrm{Tr}[M_u^{-1\dagger}(0, 0; 0, 0)]\rangle. \end{aligned} \tag{57}$$

The weight of the disconnected part is $n_f/4$ for $n_f = 2$ degenerate flavors for the state. The connected part of the correlator is identical to the full a_0 correlator.

In terms of the meson fields, the bubble correlator is (for $\tau a = tA$)

$$\begin{aligned} B_{f_0}(\vec{p}, tA) = \frac{\mu^2 A^6}{8}\sum_{\vec{y}} \exp(i\vec{p}\cdot\vec{y}A) \sum_{r,s,f,b} \sum_{r',s',f',b'} \frac{1}{2} \\ \times [\langle \phi^b_{ur,fs}(t)\phi^b_{fs,ur}(t)\phi^{b'}_{ur',f's'}(0)\phi^{b'}_{f's',ur'}(0)\rangle \\ + \langle \phi^b_{ur,fs}(t)\phi^b_{fs,ur}(t)\phi^{b'}_{dr',f's'}(0)\phi^{b'}_{f's',dr'}(0)\rangle \\ + \langle \phi^b_{dr,fs}(t)\phi^b_{fs,dr}(t)\phi^{b'}_{ur',f's'}(0)\phi^{b'}_{f's',ur'}(0)\rangle \\ + \langle \phi^b_{dr,fs}(t)\phi^b_{fs,dr}(t)\phi^{b'}_{dr',f's'}(0)\phi^{b'}_{f's',dr'}(0)\rangle]. \end{aligned} \tag{58}$$

In momentum space the correlator becomes

$$\begin{aligned} B_{f_0}(p) = \frac{\mu^2}{8A^2(L/2)^3(N_t/2)}\Bigg\{ & n_r^2 \sum_{f,b}\sum_k \left[\frac{1}{k^2 + M^2_{fu,b}} \frac{1}{(k+p)^2 + M^2_{fu,b}}\right] + 2n_r^2 \sum_b \sum_k \left[\frac{1}{k^2 + M^2_{Ub}} \frac{1}{(k+p)^2 + M^2_{Ub}}\right] \\ & - 4n_r \sum_k \left[\frac{1}{(k+p)^2 + M^2_{UI}} \frac{1}{3n_r} \frac{k^2 + M^2_{SI}}{(k^2 + M^2_{UI})(k^2 + M^2_{\eta I})}\right] - 4n_r \sum_k \left[\frac{4\delta_A}{(k+p)^2 + M^2_{UA}}\right. \\ & \left. \times \frac{k^2 + M^2_{SA}}{(k^2 + M^2_{UA})(k^2 + M^2_{\eta A})(k^2 + M^2_{\eta' A})}\right] - 4n_r \sum_k \left[\frac{4\delta_V}{(k+p)^2 + M^2_{UV}} \frac{k^2 + M^2_{SV}}{(k^2 + M^2_{UV})(k^2 + M^2_{\eta V})(k^2 + M^2_{\eta' V})}\right] \\ & + 4n_r^2 \sum_k \left[\frac{1}{3n_r} \frac{(k+p)^2 + M^2_{SI}}{[(k+p)^2 + M^2_{UI}][(k+p)^2 + M^2_{\eta I}]} \frac{1}{3n_r} \frac{k^2 + M^2_{SI}}{(k^2 + M^2_{UI})(k^2 + M^2_{\eta I})}\right] \\ & + 4n_r^2 \sum_k \left[\frac{4\delta_A[(k+p)^2 + M^2_{SA}]}{[(k+p)^2 + M^2_{UA}][(k+p)^2 + M^2_{\eta A}][(k+p)^2 + M^2_{\eta' A}]} \times \frac{\delta_A(k^2 + M^2_{SA})}{(k^2 + M^2_{UA})(k^2 + M^2_{\eta A})(k^2 + M^2_{\eta' A})}\right] \\ & + 4n_r^2 \sum_k \left[\frac{4\delta_V[(k+p)^2 + M^2_{SV}]}{[(k+p)^2 + M^2_{UV}][(k+p)^2 + M^2_{\eta V}][(k+p)^2 + M^2_{\eta' V}]} \times \frac{\delta_V(k^2 + M^2_{SV})}{(k^2 + M^2_{UV})(k^2 + M^2_{\eta V})(k^2 + M^2_{\eta' V})}\right]\Bigg\}. \end{aligned} \tag{59}$$

In terms of valence quark world lines the first five terms are quarkline connected and the last three are disconnected.

In the continuum limit we have

$$\begin{aligned} B_{f_0}(p) = \frac{\mu^2}{8A^2(L/2)^3(N_t/2)}\Bigg\{ & 16n_r^2 \sum_f \sum_k \left[\frac{1}{k^2 + M^2_{fu}} \frac{1}{(k+p)^2 + M^2_{fu}}\right] + 32n_r^2 \sum_k \left[\frac{1}{k^2 + M^2_U} \frac{1}{(k+p)^2 + M^2_U}\right] \\ & - 4n_r \sum_k \left[\frac{1}{(k+p)^2 + M^2_U} \frac{1}{3n_r} \frac{k^2 + M^2_S}{(k^2 + M^2_U)(k^2 + M^2_\eta)}\right] \\ & + 4n_r^2 \left[\frac{1}{3n_r} \frac{(k+p)^2 + M^2_S}{[(k+p)^2 + M^2_U][(k+p)^2 + M^2_\eta]} \frac{1}{3n_r} \frac{k^2 + M^2_S}{(k^2 + M^2_U)(k^2 + M^2_\eta)}\right]\Bigg\}. \end{aligned} \tag{60}$$

The two-pion threshold $(p + k)^2 + M_U^2 = 0$ and $k^2 + M_U^2 = 0$ has a weight proportional to

$$(64n_r^2 - 1)\mu^2. \tag{61}$$

When $n_r = 1/4$ the weight is 3 (for three physical pion channels). Thus, once again, only physical thresholds survive the continuum limit.

E. Single-flavor staggered fermions

Single-flavor QCD has no Goldstone bosons. The low-lying pseudoscalar (call it the η') is lifted by the anomaly. With the staggered-fermion action, however, only the taste singlet η' is lifted by the anomaly. The other 15 members of the taste multiplet (call them η) remain light. The member with pseudoscalar taste is an exact Goldstone boson. Such a spectrum would seem to spell trouble for the rooted theory. It is interesting to examine the scalar meson (f_0) correlator to see how the corresponding rooted chiral theory heals itself in the continuum limit.

Call the single replicated flavor u. The connected meson correlator is as before [Eq. (45)]. We choose not to decouple the taste singlet η' in this case because it is the only physical meson. The disconnected correlator for the taste singlet is then

$$\langle \phi^I_{gs,fr}(-k)\phi^I_{f'r',g's'}(k)\rangle_{\rm disc} = \frac{\delta_{r,s}\delta_{r',s'}\delta_{f,g}\delta_{f',g'}}{n_r} \times\left[-\frac{1}{(k^2+M^2_{UI})} + \frac{1}{k^2+M^2_{\eta' I}}\right]. \tag{62}$$

Similarly, the disconnected correlators for the taste axial vector and taste vector can be written as

$$\langle \phi^A_{gs,fr}(-k)\phi^A_{f'r',g's'}(k)\rangle_{\rm disc} = \delta_{r,s}\delta_{r',s'}\delta_{f,g}\delta_{f',g'} \times\frac{-\delta_A}{(k^2+M^2_{UA})(k^2+M^2_{\eta' A})} \tag{63}$$

and $(A \to V)$, where in this case $M^2_{\eta' A} = M^2_{UA} + n_r\delta_A$, and similarly for $M^2_{\eta' V}$.

With these changes the f_0 correlator becomes

$$\begin{aligned} B_{f_0}(p) = \frac{\mu^2}{8A^2(L/2)^3(N_t/2)}\Bigg\{ & 2n_r^2\sum_b\sum_k\left[\frac{1}{k^2+M^2_{Ub}}\frac{1}{(k+p)^2+M^2_{Ub}}\right] - 4n_r\sum_k\frac{1}{(k+p)^2+M^2_{UI}}\frac{1}{n_r}\left[\frac{1}{k^2+M^2_{UI}} - \frac{1}{k^2+M^2_{\eta' I}}\right] \\ & + 4n_r\sum_k\left[\frac{\delta_A}{[(k+p)^2+M^2_{UA}](k^2+M^2_{UA})(k^2+M^2_{\eta' A})}\right] + 4n_r\sum_k\left[\frac{\delta_V}{[(k+p)^2+M^2_{UV}](k^2+M^2_{UV})(k^2+M^2_{\eta' V})}\right] \\ & + 2n_r^2\sum_k\frac{1}{n_r}\left[\frac{1}{(k+p)^2+M^2_{UI}} - \frac{1}{(k+p)^2+M^2_{\eta' I}}\right]\frac{1}{n_r}\left[\frac{1}{k^2+M^2_{UI}} - \frac{1}{k^2+M^2_{\eta' I}}\right] \\ & + 2n_r^2\sum_k\left[\frac{\delta_A^2}{[(k+p)^2+M^2_{UA}][(k+p)^2+M^2_{\eta' A}](k^2+M^2_{UA})(k^2+M^2_{\eta' A})}\right] \\ & + 2n_r^2\sum_k\left[\frac{\delta_V^2}{[(k+p)^2+M^2_{UV}][(k+p)^2+M^2_{\eta' V}](k^2+M^2_{UV})(k^2+M^2_{\eta' V})}\right]\Bigg\}. \end{aligned} \tag{64}$$

We note that a simplified version of our result (setting the discretization corrections from δ_A and δ_V to zero) was presented previously [3]. In the continuum limit the would-be Goldstone thresholds become degenerate with the negative-norm threshold, with a net weight proportional to

$$(32n_r^2 - 2). \tag{65}$$

When $n_r = 1/4$, the would-be Goldstone bosons decouple from the f_0 correlator, leaving only the physical high-lying $\eta'\eta'$ channel.

IV. SIMULATIONS AND RESULTS

In this work we analyzed the 0.12 fm ensemble of 510 $24^3 \times 64$ gauge configurations generated in the presence of $2+1$ flavors of Asqtad improved staggered quarks with bare quark masses $am_{ud} = 0.005$ and $am_s = 0.05$ and bare gauge coupling $10/g^2 = 6.76$ [17].

We set valence quark masses equal to the sea quark masses. Table I gives the pseudoscalar masses used in our fits with the exception of the masses η_A, η'_A, η_V, η'_V. Those masses vary with the fit parameters δ_A and δ_V.

For the light quark Dirac operator M_u, we measured the point-to-point quarkline connected correlator

$$C_{\rm conn}(\vec{p},\tau) = \sum_{\vec{x}}(-)^x\cos(\vec{p}\cdot\vec{x}) \times\langle {\rm Tr}[M_u^{-1}(\vec{x},\tau;0,0)M_u^{-1^\dagger}(\vec{x},\tau;0,0)]\rangle \tag{66}$$

and point-to-point quarkline disconnected correlator

$$C_{\rm disc}(\vec{p},\tau) = \sum_{\vec{x}}(-)^x\cos(\vec{p}\cdot\vec{x}) \times\langle {\rm Tr}M_u^{-1}(\vec{x},\tau;\vec{x},\tau)\,{\rm Tr}M_u^{-1}(0,0;0,0)\rangle. \tag{67}$$

In the latter case we use noisy estimators based on random $Z(2)$ color vectors [27] η_k for $k = 1, \ldots N = 200$:

$$\begin{aligned}&\mathrm{Tr}\, M_u^{-1}(\vec{x}, \tau; \vec{x}, \tau)\, \mathrm{Tr} M_u^{-1}(0, 0; 0, 0) \\ &\approx \frac{1}{N(N-1)} \sum_{k \neq k', y, y'} \bar{\eta}_k(\vec{x}, \tau) M_u^{-1}(\vec{x}, \tau; y) \eta_k(y) \\ &\quad \times \bar{\eta}_{k'}(0, 0) M_u^{-1}(0, 0; y') \eta_{k'}(y'). \end{aligned} \tag{68}$$

In terms of these correlators the a_0 and f_0 correlators are

$$\begin{aligned} C_{a_0}(\vec{p}, \tau) &= C_{\mathrm{conn}}(\vec{p}, \tau), \\ C_{f_0}(\vec{p}, \tau) &= C_{\mathrm{conn}}(\vec{p}, \tau) - \tfrac{1}{2} C_{\mathrm{disc}}(\vec{p}, \tau). \end{aligned} \tag{69}$$

Correlators in each channel were measured at five momenta $\vec{p} = (0,0,0)$, (1,0,0), (1,1,0), (1,1,1), and (2,0,0). All ten correlators were then fit to the following model

$$\begin{aligned} C_{a_0}(\vec{p}, \tau) &= C_{\mathrm{meson}, a_0}(\vec{p}, \tau) + B_{a_0}(\vec{p}, \tau), \\ C_{f_0}(\vec{p}, \tau) &= C_{\mathrm{meson}, f_0}(\vec{p}, \tau) + B_{f_0}(\vec{p}, \tau), \end{aligned} \tag{70}$$

where

$$\begin{aligned} C_{\mathrm{meson}, a_0}(\vec{p}, \tau) &= b_{a_0}(p) \exp[-E_{a_0}(p)\tau] \\ &\quad + b_{\pi, A}(p)(-)^\tau \exp[-E_{\pi, A}(p)\tau] \\ &\quad + (\tau \rightarrow N_t - \tau), \\ C_{\mathrm{meson}, f_0}(\vec{p}, \tau) &= c_0(p) + b_{f_0}(p) \exp[-E_{f_0}(p)\tau] \\ &\quad + b_{\eta, A}(p)(-)^\tau \exp[-E_{\eta, A}(p)\tau] \\ &\quad + (\tau \rightarrow N_t - \tau). \end{aligned} \tag{71}$$

This fitting model adds explicit a_0 and f_0 poles, as well as the corresponding negative parity states, to the bubble contribution. Such states are outside the scope of the low order chiral Lagrangian in Eq. (2). Of course it is possible to enlarge the Lagrangian to include them [21]. Taste-breaking effects complicate this exercise. Moreover, we would need to introduce a variety of higher order chiral couplings, which are unlikely to be well constrained by our data. Therefore, we took the more modest approach and treated these additional terms empirically, keeping in mind the possibility of higher order chiral effects.

Our parametrization of the momentum dependence of the overlap factors $b_j(p)$ requires some discussion. The a_0 and f_0 are produced through the scalar density with spin-taste assignment 1×1. Thus at zeroth order in the $a_0 - \pi - \eta$ coupling their contributions should be inversely proportional to their energies $b_j(0) = 1/2E_j(p)$. At higher order an iteration of the bubble contribution alters the momentum dependence of the pole residue [21]. For present purposes we chose the empirical fitting form

$$b_j(p) = b_{j0} + b_{j1} p^2 \tag{72}$$

and adjusted the constants b_{j0} and b_{j1}.

The negative parity states are the taste-axial-vector pion π_A and the taste-axial-vector η_A. As staggered partners to the a_0 and f_0 they couple through axial vector currents with spin-taste assignment $\gamma_0\gamma_5 \times \gamma_0\gamma_5$, which contribute a factor of the energy to source and sink. Thus their bare momentum dependence should be proportional to their energies

$$b_j(p) = b_j E(p). \tag{73}$$

We kept this form, adjusting b_j.

The constant $c_0(p)$ is zero for all momenta except $\vec{p} = (0,0,0)$, in which case it gives the vacuum-disconnected part of the f_0 correlator. There are 11 fit parameters for the meson terms alone, but the two negative parity masses were constrained tightly by priors: the π_A, to the previously measured value, and the η_A, to the same derived mass that we used in the bubble term.

The bubble terms B_{a_0} and B_{f_0} in the fitting function Eq. (70) are given in momentum space by Eqs. (53) and (60). Their time-Fourier transforms yield $B_{a_0}(\vec{p}, \tau)$ and $B_{f_0}(\vec{p}, \tau)$ by applying the following identity term by term:

$$\begin{aligned} B(\vec{p}, \tau) &\propto \frac{1}{A^2 (N_t/2)^2} \sum_{p_0, k} \frac{e^{-ip_0 t}}{[k^2 + M_1^2][(p-k)^2 + M_2^2]} \\ &= \sum_{\vec{k}} \frac{e^{-[E_1(\vec{k}) + E_2(\vec{k})]t}}{4 E_1(\vec{k}) E_2(\vec{k})}, \end{aligned} \tag{74}$$

where $E_j(\vec{k}) = \sqrt{|\vec{k}|^2 + M_j^2}$, and, as usual, $tA \equiv \tau a$. Thus, for example, the $\bar{K}K$ contribution to $B_{a_0}(\vec{p}, \tau)$ for taste b is

$$\frac{\mu^2}{16 L^3} \sum_{\vec{k}} \frac{e^{-[E_{Kb}(\vec{k}) + E_{Kb}(\vec{k})]t}}{4 E_{Kb}(\vec{k}) E_{Kb}(\vec{k})}. \tag{75}$$

The bubble terms $B_{a_0}(p, \tau)$ and $B_{f_0}(p, \tau)$ were parametrized by the three low energy couplings $\mu = m_\pi^2/(2m_\ell)$, $\delta_A = a^4 \delta'_A$, and $\delta_V = a^4 \delta'_A$ in the notation of Ref. [15]. They were allowed to vary to give the best fit. The taste multiplet masses in the bubble terms were fixed as noted above. The sum over intermediate momenta was cut off when the total energy of the two-body state exceeded $1.8/a$ or any momentum component exceeded $\pi/(3a)$. We determined that such a cutoff gave acceptable accuracy for $\tau \geq 4$.

In summary, we fit all ten correlators with 14 parameters, eleven of which were needed to parametrize the four explicit meson terms and three low energy couplings were needed for the bubble contribution. Through a prior, we constrained the value of δ_V to conform to previous fits to the pseudoscalar masses and decay constants [15], leaving only two of the low energy couplings to be adjusted independently. Our best fit gave $\chi^2/\mathrm{dof} = 126/109$ (CL 0.13).

The fitted functional form is compared with the data in Figs. 1–3.

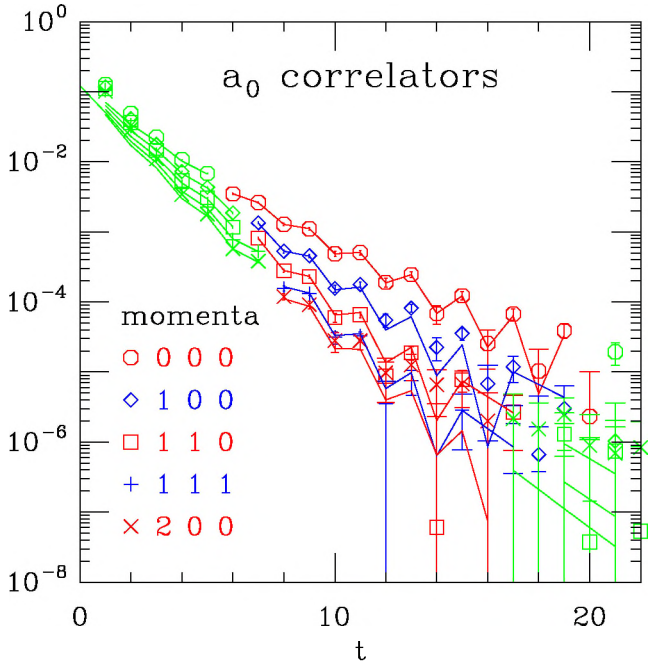

FIG. 1 (color online). Best fit to the a_0 correlator for five total cm momenta. The fitting range is indicated by points and fitted lines in red and blue (darker points and lines). Occasional points with negative central values are not plotted.

Results of the fits are compared with results from fits to the meson masses and decay constants in Table II. The agreement is worse if we used the bare value $r_1\mu = 4.5$

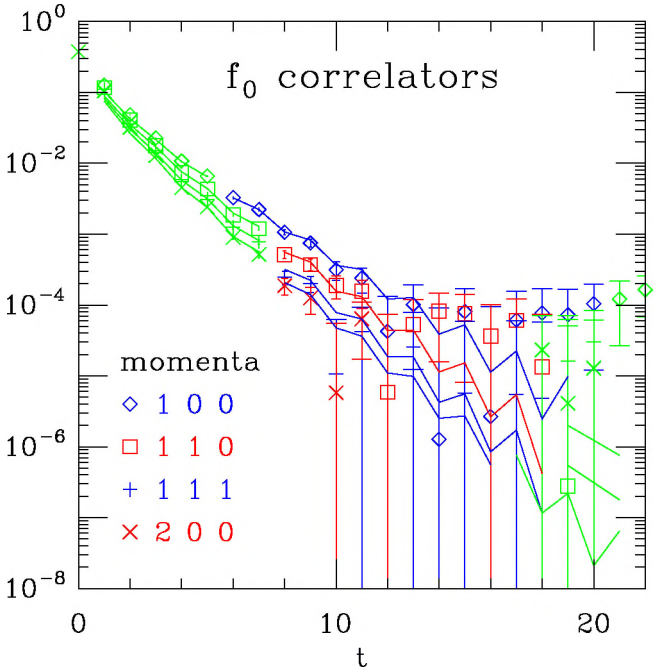

FIG. 2 (color online). Best fit to the f_0 correlator for four total cm momenta.

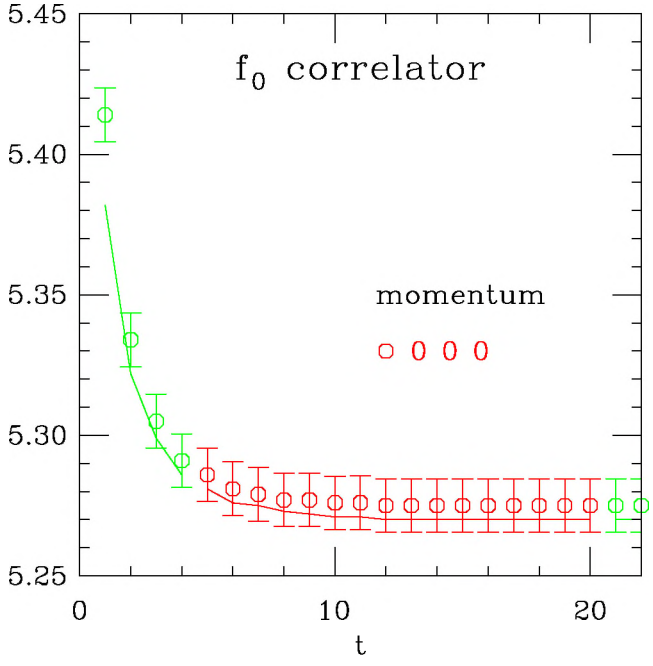

FIG. 3 (color online). Best fit to the zero momentum f_0 correlator.

from those fits, rather than the higher order $m_\pi^2/(2m_\ell)$, suggesting, perhaps, that a higher order calculation of the bubble contribution might improve the agreement.

The fitted masses of the a_0 and f_0 in units of the lattice spacing are 0.61(5) and 0.45(9), respectively.

V. SUMMARY AND CONCLUSIONS

We have derived the two-pseudoscalar-meson bubble contribution to the f_0 correlator in lowest order SχPT, thereby extending the result for the a_0 in Ref. [20]. We have used this model to fit simulation data for the point-to-point a_0 and f_0 correlators and found that best-fit values of the three chiral low energy couplings are in reasonable agreement with values previously obtained in fits to the light meson spectra and decay constants [15].

The two-meson bubble term in SχPT provides a useful illustration of the lattice artifacts induced by the fourth-root approximation, since it involves quark loops coming from the fermion determinant. The artifacts include thresholds at unphysical energies and thresholds with negative weights. These are the same sorts of artifacts commonly

TABLE II. Comparison of our fit parameters for the rSχPT low energy constants with results from [15].

	Our fit	Meson masses and decays
$r_1 m_\pi^2/(2m_{u,d})$	7.3(1.6)	6.7
δ_V	(prior)	−0.016(23)
δ_A	−0.056(10)	−0.040(6)

observed with quenching or partial quenching. These contributions are clearly present in the a_0 and f_0 channels in our QCD simulation with the Asqtad action at $a = 0.12$ fm. We have found that they must be taken into account in a successful spectral analysis. Fortunately, rSχPT provides an explicit parametrization of their contributions for the interpolating operators we have chosen, thereby allowing a fit to simulation data with a manageable number of parameters. The rSχPT predicts further that these lattice artifacts disappear in the continuum limit, leaving only physical two-body thresholds. This result is in full accordance with the fourth-root analysis of Ref. [3]. It will be interesting to see whether this expectation is borne out in numerical QCD simulations at smaller lattice spacing.

ACKNOWLEDGMENTS

This work is supported in part by the U.S. National Science Foundation, the U.S. Department of Energy, and Slovenian Ministry of Education, Science and Sport. We are grateful to the MILC Collaboration for the use of the Asqtad lattice ensemble. The analysis of these lattice files was carried out at the Utah Center for High Performance Computing.

[1] C. Bernard, M. Golterman, and Y. Shamir. Phys. Rev. D **73**, 114511 (2006).
[2] Y. Shamir, Phys. Rev. D **75**, 054503 (2007).
[3] C. Bernard, Phys. Rev. D **73**, 114503 (2006).
[4] S. R. Sharpe, Proc. Sci., LAT2006 (2006) 022.
[5] C. Bernard, M. Golterman, and Y. Shamir, Proc. Sci., LAT2006 (2007) 205.
[6] S. Durr and C. Hoelbling, Phys. Rev. D **69**, 034503 (2004).
[7] E. Follana, A. Hart, and C. T. H. Davies, Phys. Rev. Lett. **93**, 241601 (2004).
[8] S. Durr, C. Hoelbling, and U. Wenger, Phys. Rev. D **70**, 094502 (2004).
[9] S. Durr and C. Hoelbling, Phys. Rev. D **71**, 054501 (2005).
[10] E. Follana, A. Hart, C. T. H. Davies, and Q. Mason, Phys. Rev. D **72**, 054501 (2005).
[11] C. Bernard *et al.*, Proc. Sci., LAT2005 (2006) 114.
[12] C. Bernard *et al.* Proc. Sci., LAT2006 (2007) 163.
[13] C. Aubin and C. Bernard, Phys. Rev. D **68**, 034014 (2003).
[14] C. Aubin and C. Bernard, Phys. Rev. D **68**, 074011 (2003).
[15] C. Aubin *et al.*, Phys. Rev. D **70**, 114501 (2004).
[16] B. Billeter, C. DeTar, and J. Osborn, Phys. Rev. D **70**, 077502 (2004).
[17] C. Aubin *et al.*, Phys. Rev. D **70**, 094505 (2004).
[18] E. B. Gregory, A. C. Irving, C. C. McNeile, S. Miller, and Z. Sroczynski, Proc. Sci., LAT2005 (2006) 027.
[19] S. Prelovsek, Proc. Sci., LAT2005 (2006) 085.
[20] S. Prelovsek, Phys. Rev. D **73**, 014506 (2006).
[21] W. A. Bardeen, A. Duncan, E. Eichten, N. Isgur, and H. Thacker, Phys. Rev. D **65**, 014509 (2001).
[22] C. Bernard, M. Golterman, Y. Shamir, and S. R. Sharpe, Phys. Lett. B **649** 235 (2007).
[23] C. Aubin and C. Bernard, Nucl. Phys. B, Proc. Suppl. **129**, 182 (2004).
[24] W.-J. Lee and S. R. Sharpe, Phys. Rev. D **60**, 114503 (1999).
[25] C. W. Bernard *et al.*, Phys. Rev. D **64** 054506 (2001).
[26] P. H. Damgaard and K. Splittorff, Phys. Rev. D **62**, 054509 (2000).
[27] S.-J. Dong and K.-F. Liu, Phys. Lett. B **328**, 130 (1994).